

Non-Markovian dynamics of BIC generation via single-photon scattering

Giuseppe Magnifico,^{1,2} Maria Maffei,^{1,2,*} Domenico Pomarico,^{1,2}
Debmalya Das,^{1,2} Paolo Facchi,^{1,2} Saverio Pascazio,^{1,2} and Francesco V. Pepe^{1,2}

¹*Dipartimento di Fisica, Università di Bari, I-70126 Bari, Italy*

²*INFN, Sezione di Bari, I-70125 Bari, Italy*

The excitation of bound states in the continuum (BICs) in two- or multi-qubit systems lies at the heart of entanglement generation and harnessing in waveguide quantum electrodynamics platforms. However, the generation of qubit pair BICs through single-photon scattering is hindered by the fact that these states are effectively decoupled from propagating photons. We prove that scattering of a parity-invariant single photon on a qubit pair, combined with a properly engineered time variation of the qubit detuning, is not only feasible, but also more effective than strategies based on the relaxation of the excited states of the qubits. The use of tensor network methods to simulate the proposed scheme enables to include photon delays in collision models, thus opening the possibility to follow the time evolution of the full quantum system, including qubits and field, and to efficiently implement and characterize the dynamics in non-ideal cases, which turn out to be optimal for the BIC generation strategy.

Introduction.—Waveguide Quantum Electrodynamics (wQED) represents one of the most promising, feasible and versatile platforms for quantum technology implementations [1]. The opportunity of manipulating the system by tuning interaction strengths, emission frequencies, and distances between components, alongside the effectiveness of the emitter-field and the emitter-emitter couplings, guaranteed by quasi-one-dimensional field’s confinement, open the way to theoretical investigation and technological exploitation of remarkable collective phenomena [2–19]. Interesting effects already emerge in the simple case of a pair of two-level quantum emitters (qubits, henceforth), coupled to one parity-invariant waveguide mode [20–36]. Indeed, when the qubits’ distance matches specific resonance conditions, a single photon emitted from a superposition of their excited states can undergo destructive interference, giving rise to a bound state in the continuum (BIC) [37, 38]. Furthermore, in the weak coupling regime, due to the symmetry of the system, the reduced state of the qubits in the BIC is, with a good approximation, a Bell state.

Considering the existence of entangled bound states, a strategy to generate entanglement between qubits from the Hamiltonian evolution naturally follows [22, 39, 40]. A factorized initial state of the joint qubits-field system with one excited qubit and the field in vacuum partially relaxes towards the BIC. The remaining part of the state decays by emitting a photon with twice the emission rate as an isolated emitter. Such a procedure, called *entanglement by relaxation* [22], is intrinsically limited by the overlap between the initial state and the BIC and thus gives at best a probability one-half of generating the Bell state. Moreover, entanglement by relaxation becomes less and less efficient when the distance between qubits increases. When the inter-qubit distance becomes comparable with the correlation length of the spontaneously emitted field, i.e. in the so-called non-Markovian regime, the excitation gets more likely stored in a photon trapped between the qubits in a standing-wave shape [22, 31, 41, 42].

Interestingly, by adopting a change of perspective, one can harness the stationary field trapped between the qubits

to generate qubits Bell states in an alternative manner. The task of exciting a BIC through scattering is generally hindered by weak coupling and vanishing overlaps between trapped and incoming photons, thus requiring strategies such as time-dependent Hamiltonians [43] and two-photon scattering [31, 44]. In the latter case, the authors demonstrated that, in the non-Markovian regime, the BIC can be effectively excited starting from the qubits in the ground states and sending on them from one side a pulse carrying two photons. Importantly, a similar scattering-based scheme would not work if the pulse would carry just a single photon, due to the vanishing overlap between the photon states that characterize the bound state, confined between the qubits, and the initial photon state, incident from an outer region. An alternative procedure to effectively populate a BIC of distant emitters, also rooted in the two-excitation sector, is outlined in Ref. [45] where the BIC is formed via relaxation of an initially doubly excited state of the qubits.

In this Letter, we propose a method to effectively populate a two-qubit BIC in the non-Markovian regime, in the one-excitation sector, by sending *one* photon on the qubits in their ground states. As depicted in Figure 1, we bypass the aforementioned roadblock by suppressing the emitter-photon interaction until the incident photon wavefront travels the whole distance between qubits. Screening the qubit from the photon in a negligible time compared with the dynamics timescales is an experimentally feasible task (see e.g. [46, 47]); in the described procedure, we specifically refer to the possibility of detuning the qubit transition from the resonance with the scattering photon. As we will show, this strategy cures the problem of the vanishing overlap between the initial-state and the bound-state photons.

To account for non-perturbative effects in the system dynamics, we employ tensor network techniques [48–53], which provide extremely accurate numerical solutions of joint emitter-field dynamics with any number of excitation and any initial state of the propagating field also in the non-Markovian regime, where GKLS master equations for the qubits cannot be derived [54–56]. Besides not requiring any perturbative

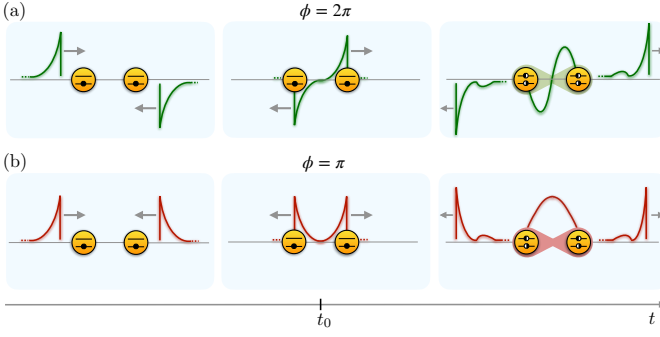


FIG. 1. Schematics of two-qubit BIC generation via single-photon scattering. From left to right, three snapshots at different stages of the proposed protocol. In both panels $\phi = \omega_0\tau$, with ω_0 being the qubits excitation frequency, and $\tau = d/v_g$ being the time that takes to the photon of speed v_g to cover the inter-qubits distance d . The system is in an even-order resonance, with $\phi = 2\pi$, in panel (a), and in an odd-order resonance, with $\phi = \pi$, in panel (b), with even and odd referring to the BIC spatial symmetry. At $t \ll t_0$, the qubits are in their ground states and decoupled from the field, while the incoming photon is prepared in a spatially antisymmetric [panel (a)] or symmetric [panel (b)] state. Until $t = t_0$, the qubits are detuned with respect to the photon. At $t = t_0$, the wavefronts of right- and left-propagating components of the incoming photon have covered the whole distance between qubits, and the latter are tuned in (detuning is turned off), getting coupled to the field. When the scattering dynamics is completed, at $t \gg t_0$, the qubits-photon system is found, with a finite probability, in a BIC containing a qubits Bell-state (resp. green and red shaded areas) with same spatial symmetry as the incoming photon.

assumption, the method allows to work directly in the time domain to tackle the scattering dynamics. Specifically, we utilized Matrix Product States (MPS) capable of reproducing the real-time evolution of the system while accounting for time-delayed continuous quantum interactions between the two qubits in the non-Markovian regime [48–50].

The results of our simulations demonstrate that the proposed scattering method strikingly outmatches the entanglement by relaxation as soon as the time for a photon to travel between the qubits becomes comparable with their lifetimes. Moreover, we show that a finite detuning value can lead to a bound state generation probability that is higher than in the ideal case of infinite detuning.

Model and dynamics.—We consider a pair of identical qubits, labelled with 1 and 2, coupled to a waveguide photon mode, and located at the points $x_1 = 0$ and $x_2 = d > 0$, respectively. In the absence of field coupling, the qubit dynamics is determined, for $j \in \{1, 2\}$, by the bare Hamiltonians

$$H_j^{(0)} = \hbar\omega_0\sigma_j^\dagger\sigma_j, \quad \text{with } \sigma_j = |g_j\rangle\langle e_j|, \quad (1)$$

where $|g_j\rangle$ and $|e_j\rangle$ are the ground and excited state, respectively, and ω_0 is the excitation frequency. For notation shortness, we will denote the tensor product basis of the qubit pair as $|ee\rangle := |e_1\rangle \otimes |e_2\rangle$, $|eg\rangle := |e_1\rangle \otimes |g_2\rangle$, $|ge\rangle := |g_1\rangle \otimes |e_2\rangle$, and $|gg\rangle := |g_1\rangle \otimes |g_2\rangle$. We assume that the field dispersion relation can be linearized, with group velocity v_g , in the fre-

quency range of interest for the system dynamics. It is convenient to define the wavenumber $k_0 = \omega_0/v_g$, corresponding to the transition frequency. We account for photon propagation in two possible directions by introducing the field operators $a_{R(L)}(\omega)$, that annihilate right(left)-propagating photons of frequency ω and wavenumber $k = +(-)\omega/v_g$. These field operators satisfy the canonical commutation relations $[a_D(\omega), a_{D'}^\dagger(\omega')] = \delta_{D,D'}\delta(\omega - \omega')$ and $[a_D(\omega), a_{D'}(\omega')] = 0$, with $D, D' \in \{R, L\}$. In terms of these operators, the bare field Hamiltonian reads

$$H_f^{(0)} = \hbar \sum_{D=R,L} \int d\omega \omega a_D^\dagger(\omega) a_D(\omega). \quad (2)$$

In the interaction picture of $H^{(0)} = H_1^{(0)} + H_2^{(0)} + H_f^{(0)}$, the emitters-field coupling Hamiltonian reads

$$V_I(t) = \hbar \sqrt{\frac{\gamma}{2}} \left\{ \sigma_1 \left[b_R^\dagger(t) + b_L^\dagger(t) \right] + \sigma_2 \left[e^{-i\phi} b_R^\dagger(t - \tau) + e^{i\phi} b_L^\dagger(t + \tau) \right] \right\} + \text{H.c.}, \quad (3)$$

where $\tau = d/v_g$ is the photon propagation time between the qubits, $\phi = k_0d = \omega_0\tau$ is the corresponding phase, and $b_D(t) = (2\pi)^{-\frac{1}{2}} \int d\omega a_D(\omega) e^{-i(\omega - \omega_0)t}$ are the quantum noise annihilation operators [57] satisfying $[b_D(t), b_{D'}^\dagger(t')] = \delta_{D,D'}\delta(t - t')$ with $D, D' \in \{R, L\}$. Equation (3) holds in the range of qubit-field couplings that lead to the validity of the rotating wave approximation and the assumption of a flat coupling over the relevant bandwidth [58, 59]. When the propagation delay τ between the qubits is much smaller than γ^{-1} , the effect of the finite propagation time between the qubits can be neglected, and their dynamics can be described by a Markovian master equation [54–56]. A further contribution to the system dynamics comes from the detuning Hamiltonian

$$H_{\text{det}}(t) = \hbar\Delta\omega(\sigma_1^\dagger\sigma_1 + \sigma_2^\dagger\sigma_2)\Theta(t_0 - t) \quad (4)$$

with $\Theta(t)$ the Heaviside step function, which is turned off at the time $t = t_0$ when the incoming photon crosses the whole inter-qubit distance (see Fig. 1).

We set a coarse-graining time interval $\Delta t \ll \gamma^{-1}$ and introduce the quantum noise increment operators, $B_{n,D} \equiv (\Delta t)^{-1/2} \int_{n\Delta t}^{(n+1)\Delta t} dt' b_D(t')$, with n being an integer, annihilating an excitation of the n -th discrete-time field mode, or *collision unit*, in the direction D [57, 60–62]. The coarse-grained evolution of the system is given by the unitary map

$$|\Psi(t_{n+1})\rangle = \exp\{-i[O_1(t_n) + O_2(t_n) + H_{\text{det}}(t_n)\Delta t/\hbar]\}|\Psi(t_n)\rangle \quad (5)$$

with

$$O_1(t_n) = \sqrt{\frac{\gamma\Delta t}{2}} \sigma_1 \left[B_{n,R}^\dagger + B_{n,L}^\dagger \right] + \text{H.c.}, \quad (6)$$

$$O_2(t_n) = \sqrt{\frac{\gamma\Delta t}{2}} \sigma_2 \left[e^{-i\phi} B_{n-\ell,R}^\dagger + e^{i\phi} B_{n+\ell,L}^\dagger \right] + \text{H.c.},$$

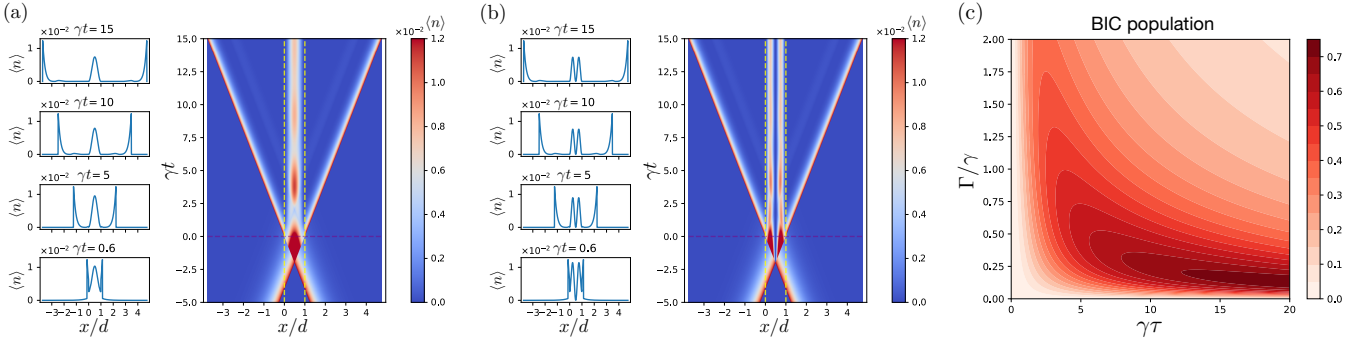


FIG. 2. Dynamics of the BIC generation via single-photon scattering. All the data are obtained by MPS numerical simulation on a lattice of 10^3 collision units, setting $\gamma\Delta t = 4 \times 10^{-2}$, and truncation error equal to 10^{-4} . (a–b) Time-evolution of the average photon number per site $\langle n(x) \rangle$, for a delay $\tau = 4\gamma^{-1}$ (with γ the excited level lifetime), for $\phi = \pi$ and initial state $|\Psi(0)\rangle = |gg\rangle \otimes |\varphi_+\rangle$ (a), and $\phi = 2\pi$ and initial state $|\Psi(0)\rangle = |gg\rangle \otimes |\varphi_-\rangle$ (b). The light-matter coupling is switched on at time $t_0 = 0$ when the right-propagating wave-front hits $x = d$ and the left-propagating one hits $x = 0$ (see Fig. 1). The incoming wavepackets have bandwidth $\Gamma = 0.625\gamma$. The insets show $\langle n(x) \rangle$ at different times during the system's evolution. (c) Asymptotic probability (final time) of populating the BIC starting from initial state $|\Psi(0)\rangle = |gg\rangle \otimes |\varphi_{(-)\ell+1}\rangle$ varying the incoming wavepacket's bandwidth and the inter-qubits delay τ of integer multiples, ℓ , of $\pi/\omega_0 = \Delta t$ such that the system is always at resonance. The plot obtained from the simulation data perfectly matches the analytical result of Eq. (9).

where the integer $\ell = \tau/\Delta t = d/(v_g\Delta t)$ is fixed by the distance d between the qubits. We notice that the map (5) couples the qubits with four different collision units at any (discrete) time of the evolution, its structure features the memory effects given by the propagation delay between the qubits: the n -th right-propagating collision unit that interacts (collides) with qubit 1 at $t = t_n$, will interact with qubit 2 at $t = t_n + \tau = t_{n+\ell}$; similarly the n -th left-propagating collision unit that interacts with qubit 1 at $t = t_n$ has already interacted with qubit 2 at $t = t_n - \tau = t_{n-\ell}$.

This non-Markovian dynamics can be efficiently simulated by means of tensor networks. In particular, the full state of the joint qubits-field system can be encoded into a collision MPS representation [48]. In this framework, a specific MPS site hosts both the qubits, whereas all the other sites encode the left- and right-propagating collision units. The implemented algorithm drives the evolution of the joint qubits-field system state once a proper initial state is initialized in the MPS form. This evolution is carried out by iteratively applying to the MPS the quantum gates that constitute the unitary map in Eq. (5). For the technical details of the algorithm and the initial state preparation, we refer to the Supplemental Material [63].

Results.— It is convenient to exploit the linearity of the dispersion relations and introduce the canonical spatial mode operators

$$c_R(x) = \frac{1}{\sqrt{v_g}} e^{-ik_0x} b_R(-x/v_g), \quad c_L(x) = \frac{1}{\sqrt{v_g}} e^{ik_0x} b_L(x/v_g), \quad (7)$$

that allow to express the BIC eigenstates [22, 31, 41, 42] at

resonance, $\phi = n\pi$, as

$$|\Phi_{\pm}\rangle = \left(1 + \frac{\gamma\tau}{2}\right)^{-\frac{1}{2}} \left[|\psi_{\pm}\rangle \otimes |0\rangle + \sqrt{\frac{\gamma}{2v_g}} |gg\rangle \otimes |1_{\text{BIC}}\rangle \right],$$

$$|1_{\text{BIC}}\rangle = \int_0^d dx \frac{e^{ik_0x} c_R^{\dagger}(x) - e^{-ik_0x} c_L^{\dagger}(x)}{\sqrt{2i}} |0\rangle, \quad (8)$$

where $|0\rangle$ is the field vacuum, $|\psi_{\pm}\rangle = (|eg\rangle \pm |ge\rangle)/\sqrt{2}$ are one-excitation Bell states of the qubit pair, and the \pm sign coincides with $(-1)^{n+1}$. Equation (8) shows that the photonic part of the BIC, $|1_{\text{BIC}}\rangle$, corresponds to a stationary field trapped between the qubits, with local energy density $\langle 1_{\text{BIC}} | c^{\dagger}(x) c(x) | 1_{\text{BIC}} \rangle = 2 \sin^2(k_0x)$, where $c(x) = c_R(x) + c_L(x)$.

In order to effectively populate the BIC starting from the qubits in $|gg\rangle$ we apply the scattering method depicted in Fig. 1. We prepare the field in a one-photon state that maximizes the overlap with the photonic part $|1_{\text{BIC}}\rangle$ of the BIC, i.e. $|\varphi_{\pm}\rangle = (|\varphi_R\rangle \pm |\varphi_L\rangle)/\sqrt{2}$ where $|\varphi_D\rangle = \int dx \varphi_D(x) c_D^{\dagger}(x) |0\rangle$ is the state of a single-photon wavepacket $\varphi_D(x)$ propagating in the direction D . In particular, we consider exponentially-shaped wavepackets $\varphi_R(x) = \sqrt{\Gamma/v_g} \Theta(d-x) \exp\{-\Gamma(d-x)/(2v_g) + ik_0(x-d)\}$ and $\varphi_L(x) = \sqrt{\Gamma/v_g} \Theta(x) \exp\{-\Gamma x/(2v_g) - ik_0x\}$. Notice that the states $|\varphi_+\rangle$ and $|\varphi_-\rangle$ have opposite symmetries with respect to the midpoint $x = d/2$ between the qubits. At time $t_0 = 0$, the wavefront of the right(left)-propagating wavepackets are in the position of qubit 2(1). The incident photon bandwidth Γ is treated as an optimization parameter. In order to exactly implement the protocol depicted in Fig. 1, one should switch on the qubits-field interaction at $t_0 = 0$. Such a condition can be realized by switching on the coupling between qubits and field at a time properly synchronized with photon arrival (see Ref. [47] for a feasible experimental implementation).

Figure 2(a-b) show the results of the MPS simulation of such scattering dynamics, obtained over a lattice of 10^3 col-

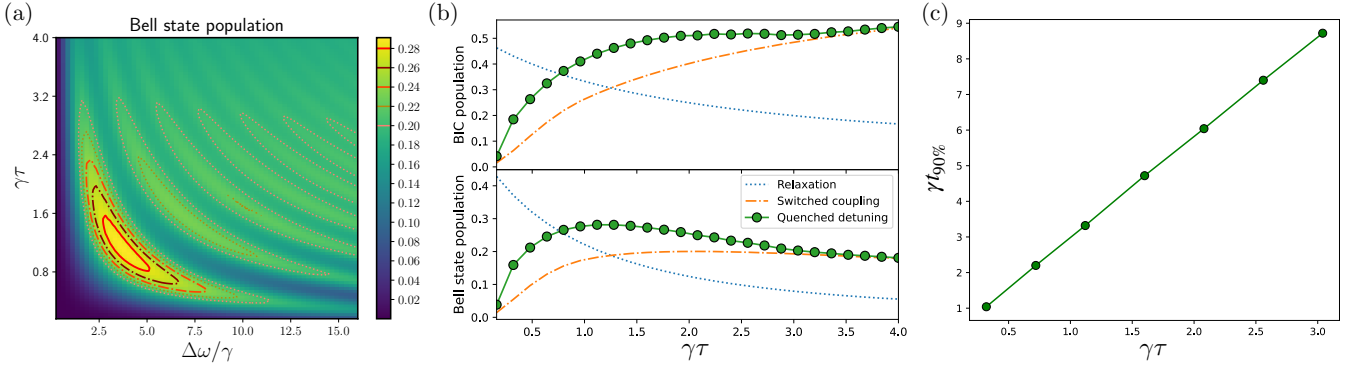


FIG. 3. Generation of the BIC via single photon scattering and quenched detuning. (a) Asymptotic (final-time) probability of populating the qubits Bell state starting from an initial state $|\Psi(0)\rangle = |gg\rangle \otimes |\varphi_{(-\ell+1)}\rangle$, obtained for different inter-qubits delays $\tau = \ell\pi/\omega_0$, with ℓ being an integer, and different values of the detuning. The value of $\Gamma\tau$ is fixed at 2.51, which maximizes the BIC population in Eq. (9) for the ideal switch case (infinite detuning). (b) Maximal asymptotic probabilities of populating the BIC and the qubits Bell states versus the inter-qubits delay (green dots). The dotted blue lines refer to the entanglement by relaxation, while the dashed orange lines represent the single-photon scattering with ideal switch of the coupling (Eq. (9)). (c) Time needed to achieve the 90% of the asymptotic BIC population with the quenched detuning method. Each point was computed by using the wavepackets bandwidth and the detuning that maximizes the Bell state population for that value of τ .

lision units, by setting the collisional coarse-graining time Δt equal to $4 \times 10^{-2}\gamma^{-1}$, and the truncation error equal to 10^{-4} . The plots show the evolution of the average photons number at each point of the x axis, i.e. $\langle n(x) \rangle \equiv \langle c^\dagger(x)c(x) \rangle$ obtained for an odd and even resonance respectively. The data show the process of standing-wave buildup between the qubits while reaching the long-time limit where it assumes a clear sinusoidal profile (see the insets), as expected from Eq. (8). The photon wavefunction that does not remain trapped in the stationary wave, is mostly transmitted forming the two main wave fronts (bright lines) that eventually reach the system's edges. The plots show also the presence of a pair of less intense wavefronts (shaded lines) due to the partial reflection of the incoming wavepackets. These reflected wavepackets travel towards the edges with a retardation from the main wavefronts equal to the delay τ and in the long-time limit (inset) form the two small bumps picked at distance d from each edge.

Figure 2(c) shows the probabilities of populating the BIC with this approach, by setting the coarse-graining time $\Delta t = \pi/\omega_0$ and varying the delay $\tau = \ell\Delta t$ by integer multiples ℓ of Δt , so that the system remains at resonance, and varying the bandwidth of the incoming field's state $|\varphi_{(-\ell+1)}\rangle$. This probability is given by the overlap (square modulus) between $|\Phi_\pm\rangle$ and the initial state $|gg\rangle \otimes |\varphi_\pm\rangle$:

$$P_{\text{BIC}} = \left| \langle \Phi_\pm | (|gg\rangle \otimes |\varphi_\pm\rangle) \right|^2 = \frac{2\gamma(1 - e^{-\Gamma\tau/2})^2}{\Gamma(1 + \frac{\gamma\tau}{2})}, \quad (9)$$

which in turn gives the qubit Bell-state population by $P_{\text{Bell}} = (1 + \gamma\tau/2)^{-1} P_{\text{BIC}}$. As expected, the overlap, i.e. the BIC population, achieved with the proposed approach, grows with the weight of the photonic part of the BIC, i.e. when the delay τ increases with respect to γ^{-1} , provided that the duration Γ^{-1} of the input pulses also increases with respect to it (i.e.

the ratio Γ/γ decreases). The probabilities are maximized by $\Gamma = \Gamma^* = 2.51/\tau$, corresponding to

$$P_{\text{BIC}}^* = 0.41 \frac{\gamma\tau}{1 + \frac{\gamma\tau}{2}}, \quad P_{\text{Bell}}^* = 0.41 \frac{\gamma\tau}{(1 + \frac{\gamma\tau}{2})^2}. \quad (10)$$

Remarkably, even though the considered optimization is performed for a particular one-parameter class of wavefunctions, the result for P_{BIC} is not far from the weight of the photon component in the BIC [see Eq. (8)], representing the absolute upper bound, that can reach 100% for large inter-qubit distances, as in the two-photon protocol proposed in Ref. [44]. Such a limit value could be reached by shaping incident square-wave photon packets with length d and appropriate symmetry, which are however harder to prepare than exponential profiles, naturally produced by decay in one dimension (see [36] for a two-qubit generalization). It is finally worth noticing that applying the same protocol represented in Fig. 1 with a photon wavepacket incoming in one direction only (i.e., either $|\varphi_R\rangle$ or $|\varphi_L\rangle$) provides a BIC excitation probability that always corresponds to $P_{\text{BIC}}/2$. Thus, despite such a one-side photon protocol is evidently sub-optimal in terms of generation probability, it is still more effective than relaxation from an excited qubit state in a certain range of $\gamma\tau$, and can be useful whenever implementing the overlap of $|\varphi_R\rangle$ and $|\varphi_L\rangle$ turns out to be unfeasible.

Though the scheme of switching the interaction is feasible in superconducting qubit platforms, the non-ideality of such a process, mostly performed through manipulation of the qubit detuning, must be taken into account. Actually, while the switch time represents a minor issue, at least for small-coupling time scales, the finite value of a realistic frequency detuning can induce significant numerical variations [46, 47]. Figure 3(a) shows the probability of populating the qubits' Bell state through a quenched detuning approach, Eq. (4), for

each value of $\gamma\tau$, by fixing the wavepacket bandwidth to the value Γ^* , which maximizes Eq. (9). Figure 3(b) shows the maximal probability of BIC and Bell state generation with quenched detuning (green dots) in comparison with the other protocols mentioned so far. The comparison of the three methods clearly shows that in the case $\gamma\tau \lesssim 1$, which includes the Markovian regime, entanglement by relaxation provides the higher probability to excite both the BIC and the qubit Bell state. For larger qubit distances, the proposed scattering approach tends to outperform the others. In particular, it is worth noticing that exploring the possibility of a quenched detuning actually allows for an improvement with respect to the ideal switch case (infinite detuning). As one can observe from Fig. 3(a), this is due to the fact that the BIC generation probability oscillates with $\Delta\omega$ around the infinite-detuning limit. From a physical point of view, the detuned Hamiltonian [Eq. (4)] prepares during the time $[t_0 - \tau, t_0]$ a more or less optimized initial state for the evolution under $H^{(0)} + V_I$ at $t > t_0$. The increase in the performance for quenched detuning remains relevant up to $\gamma\tau \lesssim 3$, where its performance becomes very close to the ideal switch case.

While the BIC excitation probability increases with the qubits distance, the probability to generate the corresponding qubits Bell state (either singlet or triplet, according to the BIC's symmetry) reaches a maximum at a finite distance. This behavior is due to the decreasing share of qubits excitation in the BIC, counterbalancing the increase in the excitation probability of the latter. Figure 3(c) displays that the time needed to achieve 90% of the asymptotic value of the Bell state population is, with very good approximation, proportional to the distance between the qubits.

Conclusions.— We proposed a scattering method to populate the one-excitation BIC that appears in the spectrum of a system of two qubits coupled to the same waveguide mode, by exploiting only the single excitation sector. The method consists in sending on the qubits in their ground states a photon with counterpropagating components, characterized by the same symmetry as the target BIC. We first investigate the case in which the interaction between qubits and field is switched on when the opposite wavefronts have covered the whole inter-qubits distance. With this protocol we find an improvement with respect to entanglement generation by relaxation, another protocol operating in the one-excitation subspace. The same procedure can be performed, in a sub-optimal but simpler way, by sending the photon only from one side, at the price of losing half of the BIC generation probability.

Our results show that, at inter-qubits distances $\tau > \gamma^{-1}$, where the system dynamics can be considered non-Markovian, the proposed method overcomes the upper limits of generation by relaxation in the one-excitation [22] and in the two-excitation sectors [45]. Being rooted in the overlap between the input photon and the photonic part of the BIC, the effectiveness of the proposed method in populating the BIC increases with the distance between qubits, as the share of field excitation in the BIC becomes larger. Interestingly, even

with a one-side photon, this method becomes more effective in populating the BIC than entanglement by relaxation, in the limit of very long delays. Then simulating the system dynamics with a MPS evolution, we characterized the performance of the process in a more realistic setting, in which the effective qubits-field interaction is controlled by a finite frequency detuning. Surprisingly, due to phase effects, the detuning can be adjusted to even outperform the result achieved in the ideal switch case, especially in the range $\tau < 3\gamma^{-1}$, thus further improving the method effectiveness.

The results obtained in this work represent the basis for a more efficient generation process of both BICs and their Bell-state components, e.g. by performing adiabatic elimination of the field. These pathways will be the subject of future research.

Acknowledgements. We acknowledge support from INFN through the project “QUANTUM” and from the Italian funding within the “Budget MUR - Dipartimenti di Eccellenza 2023–2027” - Quantum Sensing and Modelling for One-Health (QuaSiModO). PF acknowledges support from the Italian National Group of Mathematical Physics (GNFM-INDAM) and from PNRR MUR project CN00000013-“Italian National Centre on HPC, Big Data and Quantum Computing”. GM acknowledges support from the University of Bari via the 2023-UNBACLE-0244025 grant. MM, SP and FVP acknowledge support from PNRR MUR project PE0000023-NQSTI.

* maria.maffei@uniba.it

- [1] F. Ciccarello, P. Lodahl, and D. Schneble, Waveguide quantum electrodynamics, *Opt. Photon. News* **35**, 34 (2024).
- [2] C. M. Roy, D. Wilson and O. Firstenberg, Colloquium: Strongly interacting photons in one-dimensional continuum, *Rev. Mod. Phys.* **89**, 021001 (2017).
- [3] D. Lonigro, P. Facchi, S. Pascazio, F. V. Pepe, and D. Pomarico, Stationary excitation waves and multimerization in arrays of quantum emitters, *New J. Phys.* **23**, 103033 (2021).
- [4] A. Blais, A. Huang, R. S. and Wallraff, S. M. Girvin, and R. J. Schoelkopf, Cavity quantum electrodynamics for superconducting electrical circuits: An architecture for quantum computation, *Phys. Rev. A* **69**, 062320 (2004).
- [5] J. Q. You and F. Nori, Atomic physics and quantum optics using superconducting circuits, *Nature* **474**, 589 (2011).
- [6] A. Faraon, E. Waks, D. Englund, I. Fushman, and J. Vučković, Efficient photonic crystal cavity-waveguide couplers, *Appl. Phys. Lett.* **90**, 073102 (2007).
- [7] B. Dayan, A. S. Parkins, T. Aoki, E. P. Ostby, K. J. Vahala, and H. J. Kimble, A photon turnstile dynamically regulated by one atom, *Science* **319**, 1062 (2008).
- [8] E. Vetsch, D. Reitz, G. Sague, R. Schmidt, S. T. Dawkins, and A. Rauschenbeutel, Optical Interface Created by Laser-Cooled Atoms Trapped in the Evanescent Field Surrounding an Optical Nanofiber, *Phys. Rev. Lett.* **104**, 203603 (2010).
- [9] M. Bajcsy, S. Hofferberth, V. Balic, T. Peyronel, M. Hafezi, A. S. Zibrov, V. Vuletic, and M. D. Lukin, Efficient All-Optical Switching Using Slow Light within a Hollow Fiber, *Phys. Rev. Lett.* **102**, 203902 (2009).
- [10] A. Wallraff, D. I. Schuster, A. Blais, L. Frunzio, R. S. Huang,

- J. Majer, S. Kumar, S. M. Girvin, and R. J. Schoelkopf, Strong coupling of a single photon to a superconducting qubit using circuit quantum electrodynamics, *Nature* **431**, 162 (2004).
- [11] O. Astafiev, A. M. Zagoskin, A. A. Abdumalikov, Y. A. Pashkin, T. Yamamoto, K. Inomata, Y. Nakamura, and J. S. Tsai, Resonance Fluorescence of a Single Artificial Atom, *Science* **327**, 840 (2010).
- [12] J. S. Douglas, H. Habibian, C. L. Hung, A. V. Gorshkov, H. J. Kimble, and D. E. Chang, Quantum many-body models with cold atoms coupled to photonic crystals, *Nat. Photonics* **9**, 326 (2015).
- [13] U. Dorner and P. Zoller, Laser-driven atoms in half-cavities, *Phys. Rev. A* **66**, 023816 (2002).
- [14] G. Zumofen, N. M. Mojarad, V. Sandoghdar, and M. Agio, Perfect Reflection of Light by an Oscillating Dipole, *Phys. Rev. Lett.* **101**, 180404 (2008).
- [15] N. Lindlein, R. Maiwald, H. Konermann, M. Sondermann, U. Peschel, and G. Leuchs, A new 4π geometry optimized for focusing on an atom with a dipole-like radiation pattern, *Laser Phys.* **17**, 927 (2007).
- [16] H. Dong, Z. R. Gong, H. Ian, L. Zhou, and C. P. Sun, Intrinsic cavity QED and emergent quasinormal modes for a single photon, *Phys. Rev. A* **79**, 063847 (2009).
- [17] T. Tufarelli, F. Ciccarello, and M. S. Kim, Dynamics of spontaneous emission in a single-end photonic waveguide, *Phys. Rev. A* **87**, 013820 (2013).
- [18] J. T. Shen and S. Fan, Coherent Single Photon Transport in a One-Dimensional Waveguide Coupled with Superconducting Quantum Bits, *Phys. Rev. Lett.* **95**, 213001 (2005).
- [19] V. I. Yudson, Dynamics of the integrable one-dimensional system “photons + two-level atoms”, *Phys. Lett. A* **129**, 17 (1988).
- [20] A. Gonzalez-Tudela, D. Martin-Cano, E. Moreno, L. Martin-Moreno, C. Tejedor, and F. J. Garcia-Vidal, Entanglement of Two Qubits Mediated by One-Dimensional Plasmonic Waveguides, *Phys. Rev. Lett.* **106**, 020501 (2011).
- [21] E. Shahmoon and G. Kurizki, Nonradiative interaction and entanglement between distant atoms, *Phys. Rev. A* **87**, 033831 (2013).
- [22] P. Facchi, M. S. Kim, S. Pascazio, F. V. Pepe, D. Pomarico, and T. Tufarelli, Bound states and entanglement generation in waveguide quantum electrodynamics, *Phys. Rev. A* **94**, 043839 (2016).
- [23] X. H. H. Zhang and H. U. Baranger, Heralded Bell State of Dissipative Qubits Using Classical Light in a Waveguide, *Phys. Rev. Lett.* **122**, 140502 (2019).
- [24] H. Zheng and H. U. Baranger, Persistent Quantum Beats and Long-Distance Entanglement from Waveguide-Mediated Interactions, *Phys. Rev. Lett.* **110**, 113601 (2013).
- [25] C. Gonzalez-Ballester, F. J. Garcia-Vidal, and E. Moreno, Non-Markovian effects in waveguide-mediated entanglement, *New J. Phys.* **15**, 073015 (2013).
- [26] E. S. Redchenko and V. I. Yudson, Decay of metastable excited states of two qubits in a waveguide, *Phys. Rev. A* **90**, 063829 (2014).
- [27] M. Laakso and M. Pletyukhov, Scattering of Two Photons from Two Distant Qubits: Exact Solution, *Phys. Rev. Lett.* **113**, 183601 (2014).
- [28] A. F. van Loo, A. Fedorov, K. Lalumière, B. C. Sanders, A. Blais, and A. Wallraff, Photon-Mediated Interactions Between Distant Artificial Atoms, *Science* **342**, 1494 (2013).
- [29] A. Rosario Hamann, C. Müller, M. Jerger, M. Zanner, J. Combes, M. Pletyukhov, M. Weides, T. M. Stace, and A. Fedorov, Nonreciprocity Realized with Quantum Nonlinearity, *Phys. Rev. Lett.* **121**, 123601 (2018).
- [30] E. Mascarenhas, M. F. Santos, A. Auffèves, and D. Gerace, Quantum rectifier in a one-dimensional photonic channel, *Phys. Rev. A* **93**, 043821 (2016).
- [31] G. Calajó, Y.-L. L. Fang, H. U. Baranger, and F. Ciccarello, Exciting a Bound State in the Continuum through Multiphoton Scattering Plus Delayed Quantum Feedback, *Phys. Rev. Lett.* **122**, 073601 (2019).
- [32] D. Lonigro, P. Facchi, A. D. Greentree, S. Pascazio, F. V. Pepe, and D. Pomarico, Photon-emitter dressed states in a closed waveguide, *Phys. Rev. A* **104**, 053702 (2021).
- [33] P.-O. Guimond, B. Vermersch, M. Juan, A. Sharafiev, G. Kirchmair, and P. Zoller, A unidirectional on-chip photonic interface for superconducting circuits, *npj Quantum Information* **6**, 32 (2020).
- [34] M. Scigliuzzo, G. Calajó, F. Ciccarello, D. P. Lozano, A. Bengtsson, P. Scarlino, A. Wallraff, D. Chang, P. Delsing, and S. Gasparinetti, Controlling atom-photon bound states in an array of Josephson-junction resonators, *Phys. Rev. X* **12**, 031036 (2022).
- [35] S. Gasparinetti, Photons go one way or another, *Nat. Phys.* **19**, 310 (2023).
- [36] M. Maffei, D. Pomarico, P. Facchi, G. Magnifico, S. Pascazio, and F. Pepe, Directional emission and photon bunching from a qubit pair in waveguide, *Phys. Rev. Research* **6**, L032017 (2024).
- [37] F. H. Stillinger and D. R. Herrick, Bound states in the continuum, *Phys. Rev. A* **11**, 446 (1975).
- [38] H. Friedrich and D. Wintgen, Interfering resonances and bound states in the continuum, *Phys. Rev. A* **32**, 3231 (1985).
- [39] M. Gullans, T. G. Tiecke, D. E. Chang, J. Feist, J. D. Thompson, J. I. Cirac, P. Zoller, and M. D. Lukin, Nanoplasmonic Lattices for Ultracold Atoms, *Phys. Rev. Lett.* **109**, 235309 (2012).
- [40] A. Tiranov, V. Angelopoulos, C. J. van Diepen, B. Schirnski, O. A. Dall’Alba Sandberg, Y. Wang, L. Midolo, S. Scholz, A. D. Wieck, A. Ludwig, A. S. Sørensen, and P. Lodahl, Collective super- and subradiant dynamics between distant optical quantum emitters, *Science* **379**, 389 (2019).
- [41] K. Sinha, A. González-Tudela, Y. Lu, and P. Solano, Collective radiation from distant emitters, *Phys. Rev. A* **102**, 043718 (2020).
- [42] K. Sinha, P. Meystre, E. A. Goldschmidt, F. K. Fatemi, S. L. Rolston, and P. Solano, Non-Markovian Collective Emission from Macroscopically Separated Emitters, *Phys. Rev. Lett.* **124**, 043603 (2020).
- [43] Z. Hayran and F. Monticone, Capturing Broadband Light in a Compact Bound State in the Continuum, *ACS Photonics* **8**, 813 (2021).
- [44] R. Trivedi, D. Malz, S. Sun, S. Fan, and J. Vučković, Optimal two-photon excitation of bound states in non-markovian waveguide qed, *Phys. Rev. A* **104**, 013705 (2021).
- [45] W. Alvarez-Giron, P. Solano, K. Sinha, and B.-B. P., Delay-induced spontaneous dark state generation from two distant excited atoms, *arXiv preprint*, arXiv:2303.0655 (2023).
- [46] I.-C. Hoi, A. F. Kockum, L. Tornberg, A. Pourkabirian, G. Johansson, P. Delsing, and C. M. Wilson, Probing the quantum vacuum with an artificial atom in front of a mirror, *Nat. Phys.* **11**, 1045 (2015).
- [47] M. Pechal, J.-C. Besse, M. Mondal, M. Oppliger, S. Gasparinetti, and A. Wallraff, Superconducting switch for fast on-chip routing of quantum microwave fields, *Phys. Rev. Appl.* **6**, 024009 (2016).
- [48] H. Pichler and P. Zoller, Photonic Circuits with Time Delays and Quantum Feedback, *Phys. Rev. Lett.* **116**, 093601 (2016).
- [49] H. Pichler, S. Choi, P. Zoller, and M. D. Lukin, Universal pho-

- tonic quantum computation via time-delayed feedback, Proceedings of the National Academy of Sciences **114**, 11362 (2017).
- [50] P.-O. Guimond, M. Pletyukhov, H. Pichler, and P. Zoller, Delayed coherent quantum feedback from a scattering theory and a matrix product state perspective, Quantum Sci. Technol. **2**, 044012 (2017).
- [51] D. Cilluffo, N. Lorenzoni, and M. B. Plenio, Simulating Gaussian boson sampling with tensor networks in the Heisenberg picture (2024), [arXiv:2305.11215 \[quant-ph\]](https://arxiv.org/abs/2305.11215).
- [52] K. Vodenkova and H. Pichler, Continuous coherent quantum feedback with time delays: Tensor network solution, Phys. Rev. X **14**, 031043 (2024).
- [53] I. Papaefstathiou, D. Malz, J. I. Cirac, and M. C. Bañuls, Efficient tensor network simulation of multi-emitter non-markovian systems (2024), [arXiv:2407.10140 \[quant-ph\]](https://arxiv.org/abs/2407.10140).
- [54] J. Combes, J. Kerckhoff, and M. Sarovar, The SLH framework for modeling quantum input-output networks, Adv. Phys. X **2**, 784 (2017).
- [55] V. Gorini, A. Kossakowski, and E. C. G. Sudarshan, Completely positive dynamical semigroups of N-level systems, J. Math. Phys. **17**, 821 (1976).
- [56] G. Lindblad, On the generators of quantum dynamical semigroups, Commun. Math. Phys. **48**, 119 (1976).
- [57] C. W. Gardiner and P. Zoller, *Quantum Noise: A Handbook of Markovian and Non-Markovian Quantum Stochastic Methods with Applications to Quantum Optics* (Springer-Verlag, Berlin-Heidelberg, 2000).
- [58] C. Cohen-Tannoudji, J. Dupont-Roc, and G. Grynberg, *Atom-Photon Interactions: Basic Processes and Applications* (Wiley-VCH Verlag GmbH, Weinheim, 1998).
- [59] D. Burgarth, P. Facchi, R. Hillier, and M. Ligabò, Taming the rotating wave approximation, arXiv preprint arXiv:2301.02269 (2023).
- [60] F. Ciccarello, Collision models in quantum optics, Quantum Meas. Quantum Metrol. **4**, 53 (2017).
- [61] D. Cilluffo, A. Carollo, S. Lorenzo, J. A. Gross, G. M. Palma, and F. Ciccarello, Collisional picture of quantum optics with giant emitters, Phys. Rev. Research **2**, 043070 (2020).
- [62] F. Ciccarello, S. Lorenzo, V. Giovannetti, and G. M. Palma, Quantum collision models: Open system dynamics from repeated interactions, Physics Reports **954**, 1 (2022).
- [63] See supplemental material.

SUPPLEMENTAL MATERIAL

Non-Markovian dynamics of BIC generation via single-photon scattering

Giuseppe Magnifico,^{1,2} Maria Maffei,^{1,2,*} Domenico Pomarico,^{1,2}

Debmalya Das,^{1,2} Paolo Facchi,^{1,2} Saverio Pascazio,^{1,2} and Francesco V. Pepe^{1,2}

¹*Dipartimento di Fisica, Università di Bari, I-70126 Bari, Italy*

²*INFN, Sezione di Bari, I-70125 Bari, Italy*

OVERLAP BETWEEN BIC PHOTON AND INPUT PHOTON

The evaluation of the overlap between the input photon $|\varphi_{\pm}\rangle = (|\varphi_R\rangle \pm |\varphi_L\rangle)/\sqrt{2}$, with

$$|\varphi_R\rangle = \sqrt{\frac{\Gamma}{v_g}} \int dx \Theta(d-x) \exp\left\{-\frac{\Gamma}{2v_g}(d-x) + ik_0(x-d)\right\} c_R^\dagger(x)|0\rangle, \quad (S1)$$

$$|\varphi_L\rangle = \sqrt{\frac{\Gamma}{v_g}} \int dx \Theta(x) \exp\left\{-\frac{\Gamma}{2v_g}x - ik_0x\right\} c_L^\dagger(x)|0\rangle, \quad (S2)$$

and the BIC photon component in Eq. (8) determines the BIC generation probability P_{BIC} in the case of ideal interaction switch:

$$\begin{aligned} \langle \Phi_{\pm}|gg\rangle \otimes |\varphi_{(-)^{n+1}}\rangle &= -\frac{i}{2v_g} \sqrt{\frac{\Gamma\gamma/2}{1+\frac{\gamma\tau}{2}}} \int_0^d dx \left\{ \exp\left[-\frac{\Gamma}{2v_g}(d-x) - ik_0d\right] - (-)^{n+1} \exp\left[-\frac{\Gamma}{2v_g}x\right] \right\} \\ &= -i \sqrt{\frac{\gamma}{2\Gamma(1+\frac{\gamma\tau}{2})}} \left(1 - e^{-\frac{\Gamma\tau}{2}}\right) (e^{ik_0d} + (-)^n). \end{aligned} \quad (S3)$$

Therefore, in the resonance cases when $k_0d = n\pi$, the overlap between the BIC $|\Phi_{(-)^{n+1}}\rangle$ and the photon with the same spatial symmetry reads

$$P_{\text{BIC}} = |\langle \Phi_{(-)^{n+1}}|gg\rangle \otimes |\varphi_{(-)^{n+1}}\rangle|^2 = \frac{2\gamma}{\Gamma(1+\frac{\gamma\tau}{2})} \left(1 - e^{-\frac{\Gamma\tau}{2}}\right)^2, \quad (S4)$$

while the overlap with $|gg\rangle \otimes |\varphi_{(-)^n}\rangle$ vanishes. Using the above results, it is also immediate to verify that, whenever $|\Phi_{\pm}\rangle$ is a BIC,

$$|\langle \Phi_{\pm}|gg\rangle \otimes |\varphi_R\rangle|^2 = |\langle \Phi_{\pm}|gg\rangle \otimes |\varphi_L\rangle|^2 = \frac{\gamma}{\Gamma(1+\frac{\gamma\tau}{2})} \left(1 - e^{-\frac{\Gamma\tau}{2}}\right)^2 = \frac{P_{\text{BIC}}}{2}. \quad (S5)$$

TENSOR NETWORK METHODS

The MPS scheme for non-Markovian collision models is based on the iterated application of the unitary map in Eq. (5), depicted in Figure 1 [1]. The most difficult operation for the application of collision model

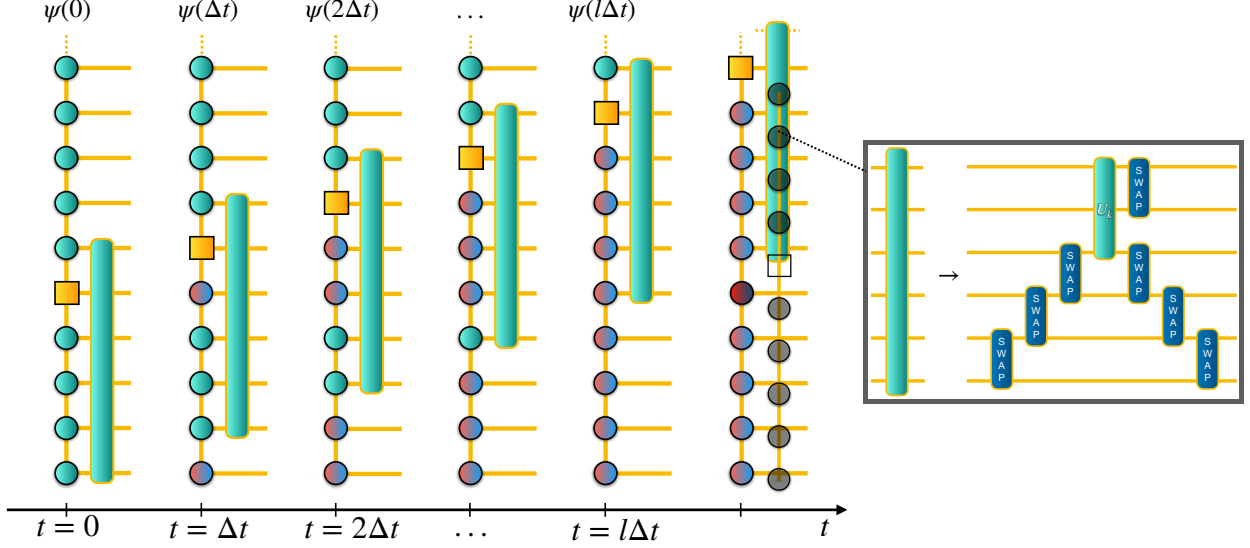


FIG. 1. Tensor Network implementation of the system dynamics.

techniques is referred to the long coupling expressed in Eq. (6), targeted in tensor network methods by means of *SWAP* gates as explained in the inset of Figure 1.

The time evolution simulation is based on the definition of a time bins lattice, conveniently modeled in the considered single-excitation sector as a qubit pair per site. Such qubits are not referred in this framework to the two-level emitters undergoing the possible formation of a BIC, but just as a truncated way to host bidirectional photons propagating through the waveguide. Let us consider a unidirectional (or equivalently known as chiral) waveguide, such that each time bin hosting photons can be modeled as a single qubit. If we assume that the propagation is towards the left (L), we can express an input photon $|\xi_L\rangle = \Xi|0\rangle$ in terms of a Matrix Product Operator (MPO)

$$\Xi = W^{[1]}W^{[2]} \dots W^{[N]}, \quad (S6)$$

defined in an analogous way in [2], where N is the number of sites composing the lattice and each operator-valued matrix reads

$$W^{[1]} = \begin{pmatrix} \xi(1)\sigma_{L,1}^+ & \mathbb{1}_2 \end{pmatrix}, W^{[s]} = \begin{pmatrix} \mathbb{1}_2 & 0 \\ \xi(s)\sigma_{L,s}^+ & \mathbb{1}_2 \end{pmatrix} \text{ for } s = 2, \dots, N-1, W^{[N]} = \begin{pmatrix} \mathbb{1}_2 \\ \xi(N)\sigma_{L,N}^+ \end{pmatrix}, \quad (S7)$$

yielding $|\xi_L\rangle = \sum_s \xi_L(s)\sigma_{L,s}^+|0\rangle$, with $\mathbb{1}_2$ standing for a 2×2 identity matrix. The wave packet is then propagated by applying the evolution represented in Figure 1, where circle sites host photonic amplitudes, while the yellow square site is referred to the two-level emitters pair, also implemented as a qubit pair like in the aforementioned bidirectional case. Within each time step a sequence of *SWAP* gates brings the photonic site placed at the time delay distance ℓ at the nearest-neighbor position with respect to the yellow

square site, then the unitary map in Eq. (5) acts on three contiguous lattice sites. After the interaction another sequence of *SWAP* gates brings back the photonic site at the time delay position, while a single *SWAP* gate moves the emitters yellow square site through the photonic lattice. We repeat this recipe until the emitters site reaches the lattice boundary.

* maria.maffei@uniba.it

- [1] H. Pichler and P. Zoller, Photonic Circuits with Time Delays and Quantum Feedback, *Phys. Rev. Lett.* **116**, 093601 (2016).
- [2] D. Cilluffo, N. Lorenzoni, and M. B. Plenio, Simulating Gaussian boson sampling with tensor networks in the Heisenberg picture (2024), [arXiv:2305.11215](https://arxiv.org/abs/2305.11215) [quant-ph].